Formulation and Evaluation of Protein Based Nano Particulate System For Treatment of Pulmonary Infections

Praveen Tahilani*[1], Hemant Swami[2], Nirmal Dongare[2]

1. Research Scholar, Institute of Pharmaceutical Sciences, SAGE UNIVERSITY Indore, M.P.
2. Professor, Institute of Pharmaceutical Sciences, SAGE UNIVERSITY Indore, M.P.

ABSTRACT

In addition to the so-called *small molecule drugs*, proteins and peptides are of increasing interest for pharmacotherapy, due to several advantageous properties. In general, those compounds are administered parenterally. However, non-invasive routes of administration represent a great part of research. Amongst others is the pulmonary application of proteins and peptides for local delivery in the case of pulmonary diseases, such as idiopathic pulmonary fibrosis, where the alveolar epithelium is affected. To ensure an intracellular delivery, nanoparticles in a size range of 150 nm were prepared *via* charge-mediated coacervation, characterized for their physicochemical properties and loaded with several model-proteins and -peptides. The material used for nanoparticle preparation was chosen to be positively and negatively charged starch derivatives, which were synthesized from potato starch. Although nanoparticles in that size range are known to show an increased cell uptake, they do not show a high deposition in the deep lung. Thus, an advanced carrier system consisting of a fast dissolving microparticle matrix with embedded starch nanoparticles was developed and characterized. Due to its aerodynamic properties, that carrier system was able to deposit a high fraction of the applied dose in the deep lung (~50%), while at the same time demonstrating (in *in vitro* models) the ability to facilitate uptake of starch nanoparticles into cells of the alveolar epithelium after fast dissolution of the microparticle matrix.

Keywords: Protein Based Nano Particulate, *In vitro* models, coacervation

*Corresponding Author Email: tahilanipraveen@gmail.com

INTRODUCTION

The pulmonary application of proteins and peptides is a promising non-invasive route of administration[1]. Systemic delivery *via* the lungs is an interesting approach as a large absorptive surface area, a high vascularization and a thin air-blood-barrier support the uptake of APIs from this site[2]. Additionally, the avoidance of the first-pass effect, known to be present in the case of oral delivery, shows further advantages for pulmonary administration.[1] Local delivery to the lungs may also present a number of benefits, and as such, COMPACT has chosen local lung delivery as one of their preferred routes of administration[3]. This is of importance for diseases such as asthma, chronic obstructive pulmonary disease (COPD), lung cancer, cystic fibrosis (CF), idiopathic pulmonary fibrosis (IPF) and pulmonary infections[4]. The direct application to the site of action is favored, due to reduced systemic side effects and a rapid onset of action[5]. The actual target of course depends on the disease, and was chosen in the context of COMPACT to be the alveolar epithelium. This site is heavily affected in IPF, in which repeated cycles of epithelial cell injury may lead to an activation of alveolar epithelial cells, resulting in an abnormal wound repair with exaggerated accumulation of fibroblasts and extracellular matrix[6]. A first model drug, that could actually function as API in the context of IPF is the intracellularly-active peptide Nrf-2.[25-30] Achieving uptake of such a peptide into non-phagocytic, epithelial cells is however considerably more challenging compared to *e.g.* macrophages, which are known to engulf nearly everything (in accordance with their physiological function).[7] The previously developed nanoparticle formulation shows a good size range suitable for the uptake into epithelial cells of the deep lung, which requires nanoparticle carriers below 200 nm in size[22-23]

Amongst other factors, the deposition of particles in the lung is influenced by the physical and chemical properties of the particles, which can be easily addressed, by controlling the preparation parameters of the particles.[8] It is known, that particle deposition occurs due to three major mechanisms: impaction, sedimentation and diffusion.[11-15] Very large particles (> 8 µm d_{aero}) deposit already in the mouth and throat[9]. Medium sized particles (d_{aero} ~ 4 - 10 µm) tend to deposit in the bronchioles, whilst smaller particles (20-50 nm < d_{aero} < 2-5 µm) deposit in the alveolar region.[16-21,24] As can be seen, the size of developed nanoparticles (~150 nm) is not ideally suited for respiration[32] and delivery to the deep lung[10].

Thus, the previously developed formulation needs further optimization in order to allow for efficient deposition in the deep lung. Besides applying APIs by nebulizers, and metered dose inhalers (MDI), dry powder inhalers (DPI) are favored. These systems show numerous advantages,

being propellant-free, portable and easy to operate, and showing an improved stability of the formulation as a result of existence in a dry state.[31-35]

Spray drying is a mild, commonly used method for preparation of dry powders.[18, 14] It has been applied to a variety of substances, such as antibiotics,[15] vaccines,[16] and peptides.[17] The Nano Spray Dryer (Büchi B-90) is furthermore a good choice, as it is known to facilitate the preparation of particles in a size range of a few μm, interesting for deep lung delivery. Different particle types can be produced by spray drying. Hollow Trojan microparticles, as prepared by Tsapis *et al.*, consist of a NP layer building the microparticle.[10] Various porous particle types were introduced by Yang *et al.*[18] and Ungaro *et al.*[19] Also matrix particles are known, where the nanoparticles are embedded in a microparticle matrix.[18, 11]

An advanced carrier system was designed for deep lung deposition of nanoparticles developed as nano- in microparticle dry powder formulation. This system was proposed to a) escape macrophage clearance and b) mediate alveolar epithelial cell uptake of the NPs. Selection of excipients used for microparticle formation was made based on their possession of high water solubility. Consequently, in this chapter, the advanced carrier system for pulmonary application was prepared from CS and Starch NPs, spray dried with different excipients, *i.e.* lact, treha, and manni. Various characterization methods were used to assess the properties of the microparticles: the most important investigation being the redispersion behavior of NPs after disintegration of the microparticles, followed by assessment of morphology, powder crystallinity, and localization of NPs in the microparticles, as well as particle size, and aerodynamic properties.

MATERIALS AND METHOD

Materials

Partially hydrolyzed potato starch (M$_W$ 1 300 000 g/mol, approx. 33% amylose content) was a gift from AVEBE. Negatively (NegSt) and positively (PosSt) charged starches were synthesized in house. Chitosan UP CL 113 (CS) was bought from NovaMatrix. Sodium tripolyphosphate (TPP) was purchased from Merck. IgG1 was kindly donated by Boehringer Ingelheim. Mannitol, trehalose dihydrate and α-lactose monohydrate (lact) were bought from Sigma Aldrich. G-Blocks (guluronic acid oligomers, consisting of more than 90% guluronic acid residues and some mannuronic acid residues, dp10 and d22) were a kind gift from the Department of Biotechnology, Norwegian University of Science and Technology (NTNU). Alexa Fluor 647 carboxylic acid (succinimidyl ester) and Bodipy FL-C5 NHS Ester (succinimidyl ester) were obtained from Life Technologies. Purified water was produced by a milliQ water purification system (Merck Millipore). All other reagents were of analytical grade.

Preparation of Microparticles

Preparation and Loading of Chitosan Nanoparticles

CS NPs were prepared by ionic gelation of positively charged amine groups of CS with negatively charged phosphate groups of TPP in aqueous solution, in a procedure adapted from Calvo *et al.*[13] Besides material concentration, the molar ratio of components, as well as the stirring speed (500 rpm, 1000 rpm) and injection rate (5 mL/min, 10 mL/min, 20 mL/min) for particle preparation using a syringe pump were investigated, as parameters potentially influencing the characteristics of resulting NPs. Further, the impact of the preparation medium was explored, by utilizing either purified water, or 10 mM HOAc/OAc$^-$ buffer pH 5.0 with and without different amounts of NaCl (5 mM, 10 mM, 50 mM). Briefly, materials were dissolved in aqueous medium to obtain solutions of 1 mg/mL, 0.5 mg/mL and 0.25 mg/mL and filtered. Different molar ratios (20:1, 10:1, 2:1 and 0.5:1) of CS:TPP were studied by adding adequate volumes of TPP solutions (1, 0.5, 0.25 mg/mL) to CS solutions (1, 0.5, 0.25 mg/mL) under gentle stirring at RT. NPs formed spontaneously and were analyzed after 10 min of stirring for equilibration. The final pH value of all tested formulations was 5.0.

In order to assess the use of CS NPs as DDS for proteins, five proteins varying in size and net charge, were chosen for loading experiments. These proteins were IgG1 (Mw: 150 kDa, isoelectric point (IEP): 8.5), BSA (Mw: 66 kDa, IEP: 4.7), OVA (Mw: 44 kDa, IEP: 4.5), Lyso (Mw: 14 kDa, IEP: 11.4) and Nrf2 (Mw: 1.3 kDa, IEP: 3.5). For the loading experiments, each protein sample was prepared as 5 mg/mL stock solution in purified water and added in various concentrations to the NP suspension to obtain final protein concentrations of 10.4 µg/mL, 20.7 µg/mL, and 41.3 µg/mL.

Preparation and Loading of Starch Nanoparticles

Starch NPs were prepared by charge-mediated coacervation between negatively charged carboxylate groups (NegSt) and positively charged amine groups (PosSt) of α-starch derivatives in aqueous solution. Briefly, materials were dissolved in purified water to obtain solutions of 1 mg/mL, 0.5 mg/mL, and 0.25 mg/mL, and filtered. Different molar ratios (3:1, 1:1, 1:3) of PosSt and NegSt solutions were studied by adding adequate volumes of NegSt (1, 0.5, 0.25 mg/mL) solution to PosSt solution (1, 0.5, 0.25 mg/mL) under gentle stirring at RT. NPs formed spontaneously and were analyzed after 10 min of stirring for equilibration. The final pH value was 7.4 for all tested formulations.

For later characterization studies of the formulation as well as uptake studies, labeled starch NPs were prepared from solutions of 0.25 mg/mL and a molar ratio of 1:1 of PosSt: NegSt. Instead of

PosSt alone, different mass ratios of PosSt: PosStF (100:0, 50:50, 10:90, 5; 95) were used for particle preparation.

Four proteins varying in net charge and size were chosen for loading experiments, in order to assess the use of starch NPs as DDS. In detail, these proteins were vanco (Mw: 1.5 kDa, IEP: 7.5), Paclitaxel, RNAse A (Mw: 14 kDa, IEP: 9.6), and IgG1 (Mw: 150kDa, IEP: 8.5). Each protein sample was prepared as 5 mg/mL stock solution in purified water and added to the NP suspension to obtain final protein concentrations of 17.2 µg/mL, 34.2 µg/mL, and 51.2 µg/mL.

Scale-up of nanoparticle preparation

For upscaling of CS NPs, the preparation was performed as described earlier, but with an increased volume: NP formation therefore occurred spontaneously after adding 10 mL of TPP solution to 50 mL of CS solution under stirring at 300 rpm (molar ratio 10:1, CS:TPP). The final pH value was 5.5.

Up scaling of starch NPs was also facilitated by an increase of volume: 20 mL of NegSt were added to 20 mL of PosSt under stirring at 700 rpm (molar ratio 1:1). The final pH value was 7.4. For loaded starch NP samples, 150 µL of IgG1 solution (5 mg/mL) was added to 40 mL of starch NP suspension. Stirring speed and injection rate were adjusted for both CS and starch NP formulation.

Microparticle preparation

Either blank NP suspension or NP suspension with excipient was spray dried with a nano spray dryer (Büchi B-90, Büchi, Switzerland). Lact, treha or manni was added to the NP suspension prior to spray drying, in mass ratios of NP: excipient 1:5, 1:10 and 1:20. Additionally, the influence of microparticle matrix forming G-Blocks (dp10, dp22) on the physicochemical properties of NP suspensions was tested. Different spray caps (4 µm, 5.5 µm and 7 µm) and inlet temperatures (90 °C, 70 °C, and 50 °C) were investigated for spray drying. The spray dryer was equilibrated with water prior to every spray drying run. The spray drying process for further particle analysis was performed at 70 °C inlet temperature, an outlet temperature of maximum 40 °C and a gas flow of 130 L/min, using the 5.5 µm spray cap. The spray rate was always 100% and samples - typical batch size was 40 or 50 mL feed volume - were kept on ice during the spray drying process. For NGI experiments, 10 µL sodium fluorescein solution (FluNa, 5 mg/mL) was added to each sample and spray drying was performed under light protection. Samples were stored in a desiccator until usage.

NANOPARTICLE RELEASE FROM MICROPARTICLES

Release of NPs from the microparticles matrix was tested in a proof of concept study by dissolving approximately 1 mg of microparticles in 1 mL of purified water. After 10 s vortexing, the particle size and PdI of released NPs was determined by Dynamic Light Scattering using the Zetasizer Nano ZSP (Malvern Instruments, UK) with a scattering angle of 173 °.

Morphology

Morphology of microparticles was examined by SEM (JSM 7001F Field Emission SEM (Jeol, Japan)). Samples were immobilized on a carbon disc and sputtered with gold (layer thickness approx. 10 nm) prior to scanning. The accelerating voltage was 5 kV. In case of the Pharmaceutical Aerosol Deposition Device on Cell Cultures (PADDOCC) deposition study, samples were directly deposited on SEM carbon discs and analyzed as mentioned above.

Particle Size Distribution

Particle size distribution was determined by image analysis of SEM images, using the Fiji Software (Fiji is a distribution of Image J available at http://fiji.sc). Particle sizes were measured, grouped into different intervals and plotted as number of particles [%]. More than 100 particles were analyzed per image. Additionally, particle size distribution was analyzed by static laser light diffraction using the HORIBA LA-950 (HORIBA, Japan) powder feeder attachment. Vibration and air suction allowed the powder to pass through a laser light beam and to be analyzed directly as dry powder without the need of applying a non-solvent.

Powder Crystallinity

For X-ray powder diffraction (XRPD) experiments, samples were analyzed by a diffractometer of the type Bruker D8 Advance, equipped with an 1D-detector 'Lynxeye' using variable divergence slit and Cu-Kα radiation. X-ray diffraction is based on radiation scattering and interference. Diffraction occurs when light is scattered by a periodic array with long- range order, producing constructive interference at specific angles. The scattering of X-rays from atoms produces a diffraction pattern, which contains information about the atomic arrangement within the crystal. The conditions for constructive interference are described by Braggs Law, where n is the order of the diffracted beam, λ is the wavelength of the x-ray radiation, d is the distance between the parallel lattice planes from which the waves are scattered and θ is the angle between the x-rays and the lattice plane:[45-50]

$$n * \lambda = 2 * d * sin\theta$$

According to Bragg's law, constructive interference for a set of atomic planes with d-spacing only occurs when the incident angle is θ. When the scattered waves interfere constructively,

they remain in phase, as the path length of each wave is equal to an integer multiple of the wavelength. Such an occurrence yields a peak in the diffractogram.

The position and intensity of peaks in a diffraction pattern are determined by the crystal structure. The absence of peaks in the diffractogramz or the presence of so-called halos indicates a completely amorphous material, which does not have a periodic array with long- range order, and so does not produce a diffraction pattern.[43]

Localization of Nanoparticles in Microparticles

The internal composition of the carrier system was observed by a confocal laser scanning microscope (Zeiss LSM710, Zeiss, Germany). Lasers at 405 nm (4′,6-Diamidino-2- phenylindole, DAPI), 488 nm (starch NPs) and 633 nm (IgG1) were used for detection. Labeled starch NPs were spray dried with treha (mass ratio 1:20) and DAPI (12.5 ng/mL). For loaded particles, 150 µL labeled IgG1 (5 mg/mL) was added to the labeled starch NP suspension beforehand. Aliquots of the spray dried powders were fixed on a glass slide. Confocal images were analyzed using the Zen 2012 software (Carl Zeiss Microscopy GmbH). IgG1 was labeled with Alexa Fluor 647 carboxylic acid (succinimidyl ester) according to the manufacturers' protocol (life technologies, USA). Purification was performed with PD-10 Desalting Columns (GE Healthcare, UK).

Aerodynamic Properties

The mass median aerodynamic diameter (MMAD), the geometric standard deviation (GSD), and the fine particle fraction (FPF) of microparticles prepared by spray drying of NPs with excipient in a mass ratio 1:20 and 10 µL FluNa (5 mg/mL) for analysis were determined with the Next Generation Impactor (NGI). For NGI experiments, the flow rate was adjusted to 60 L/min and the time of aspiration was set to 4 s. The powder inhaler (Handihaler®, Boehringer Ingelheim, Germany) was loaded with a hard gelatin no.3 capsule, filled with 10 mg of powder (n = 3). After inhaler actuation, particle deposition on the NGI was determined by correlating fluorescence intensity to deposited mass. Therefore, a standard curve was prepared from each sample and fluorescence intensity was measured at λ_{ex}= 485 nm and λ_{em} = 530 nm. The fluorescent dye FluNa was equally distributed throughout the formulation. FPF is defined as the part of the inhaled dose with an aerodynamic diameter < 5 µm in %. Further important parameters are the MMAD and the GSD. The MMAD is correlated to the detected mass within the NGI and is the mass median aerodynamic diameter, meaning that 50% of the particles are smaller than this value and 50% are larger. The GSD gives an idea of the particle distribution.

PADDOCC Deposition

The deposition of microparticles was studied with the help of the PADDOCC (Pharmaceutical Aerosol Deposition Device on Cell Cultures), which is a deposition device for dry powder, developed in-house.[41-49] Deposition behavior and morphology was analyzed after direct deposition on carbon disc wafers, by SEM. Particle deposition was determined quantitatively by correlating fluorescence intensity to deposited mass. For quantification, microparticles, co-spray dried with FluNa were used; a standard curve was prepared from each sample and fluorescence intensity was measured at λ_{ex}= 485 nm and λ_{em} = 530 nm.

RESULTS AND DISCUSSION

Preparation of Microparticles

Scale-up of nanoparticle preparation

For preparing the microparticles from the NP suspension *via* spray drying, the preparation method of NPs was up-scaled. As an increase in concentration of the solutions led to an increased size of the NPs , the process was up-scaled by increasing the volume but keeping the concentration constant at 0.25 mg/mL. Different beaker types and injection rates were tested and the impact on physicochemical properties of NPs is shown in Table 1.

Both NP types showed a size around 150 nm, with a narrow particle size distribution. They differed, however, in their ζ-potential, with CS NPs showing a positive ζ-potential of approximately +35 mV and starch NPs showing a negative ζ-potential of approximately -20 mV.

It could be concluded that the NP preparation process was suitable for up-scaling by increasing the volume. However, a good solvent mixture has to be assured, by selection of a suitable beaker type, magnetic stirrer and injection rate, depending on the kind of syringe to be employed in the preparation process. Following investigation and control of these process parameters, the physicochemical properties of NPs stayed constant as compared to the original preparation process.

Table 1: Characteristics of NPs in process upscaling studies prepared from 0.25 mg/mL solutions and a molar ratio of 1:1 (PosSt:NegSt) and 10:1 (CS:TPP) with varying process parameters; bold: formulations used for microparticle preparation. Beaker type 1123: 150 mL; beaker type 1122: 100 mL; beaker type 1169: 50 mL; all from VWR, USA).

Beaker type	Syringe volume [mL]	Injection rate [mL/min]	Size [d.nm]	PdI	ζ-potential [mV]
CS NPs					
1122	10	30	175.9 ± 1.5	0.159	$+35.1 \pm 0.9$
1122	20	60	199.0 ± 1.5	0.163	$+35.2 \pm 0.5$
1123	10	20	136.1 ± 0.4	0.151	$+35.5 \pm 2.8$
Starch NPs					

1169	20	20	180.8 ± 1.5 0.055-19.5 ± 1.3
1169	20	40	157.9 ± 1.6 0.071-17.9 ± 2.3
1169	20	60	145.1 ± 0.7 0.066-18.1 ± 3.5

Microparticle preparation

Microparticles were prepared from aqueous CS NP or starch NP suspensions (Table 1, bold) spray dried with a nano spray dryer with or without different excipients. An influence of the spray cap on the size of microparticles was disproved and the 5.5 µm spray cap was chosen for all following experiments. To ensure a dry product while at the same time ensuring mild preparation conditions feasible for protein encapsulation, an inlet temperature of 70 °C was selected. Although this temperature seems to be quite high, the most important temperature influencing product stability is in fact the outlet temperature, which was always below 40 °C in this case. To further ensure a mild preparation process, samples were kept on ice during spray drying. To determine NP stability during the pumping process, physicochemical properties of NPs were determined before spray drying and almost at the end of the spray drying process by taking samples from the remaining NP suspension. Size and ζ- potential of NPs remained the same prior to and at the end of spray drying, meaning that the pumping process as well as temperature differences did not influence particle properties over the duration of the spray drying process, which usually took approximately 2 – 2.5 h for the applied volumes.

NP suspensions were spray dried with excipient; therefore, the influence of the excipient on physicochemical properties of NPs was investigated. Here, a focus was placed on excipients that were highly water soluble, in order to easily release the NPs after deposition in the deep lung. Further, excipients with GRAS status were favored, resulting in a choice of excipients being lact, treha, and manni. Solid excipient was either added after NP preparation and stirred for 10 min for equilibration, or NPs were directly prepared in excipient solution. For the latter, each material for NP preparation (*i.e.* CS, TPP, NegSt, PosSt) was dissolved in an excipient solution instead of purified water. As no differences between the two preparation methods was observed, it was decided to add the solid excipient after NP preparation. The influence of excipients on physicochemical properties of NPs can be found in Table 1.2. As can be seen, the addition of excipients, *i.e.* manni, lact, and treha did not change the physicochemical properties of NPs. Particles were in general around 150 nm with a PdI of around 0.16 for CS NPs and 0.07 for starch NPs. The ζ-potential was approximately +35 mV and -25 mV for CS NPs and starch NPs, respectively.

Table 2: Influence of excipient on physicochemical properties of NPs, after applying to the NP suspension as dry powder; measured after stirring for 10 min for equilibration. Dp10 and dp22 are G-Blocks, with the number indicating their oligomer length. Manni: mannitol, lact: lactose, treha: trehalose.
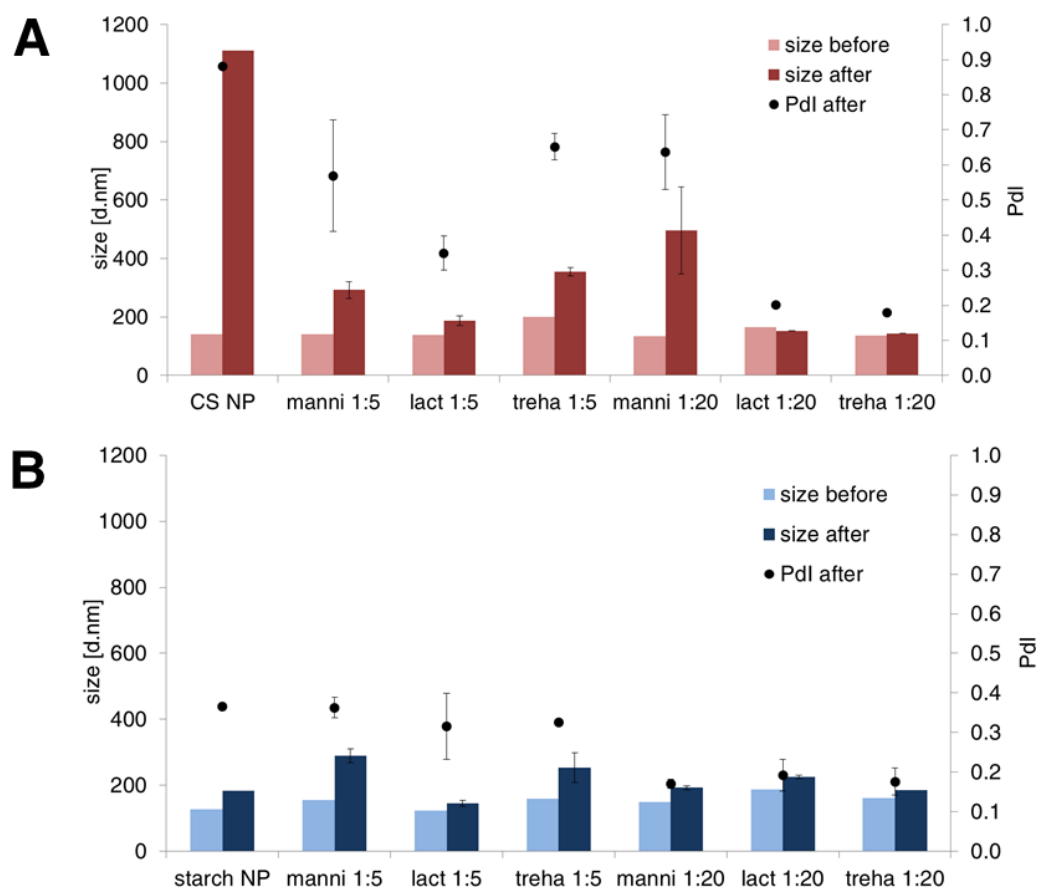
	Size[d.nm]	PdI	ζ-potential[mV]
CS NPs + manni 1:20	149.4 ± 1.9	0.171	+37.1 ± 1.4
CS NPs + lact 1:20	150.3 ± 1.5	0.175	+36.6 ± 0.9
CS NPs + treha 1:20	135.9 ± 1.5	0.152	+36.4 ± 1.2
Starch + manni 1:20	153.3 ± 0.4	0.085	-23.0 ± 0.2
Starch + lact 1:20	152.7 ± 1.9	0.065	-23.4 ± 0.3
Starch + treha 1:20	154.1 ± 1.5	0.083	-23.6 ± 0.8
CS + dp22 1:0.4	588.5 ± 120.7	0.733	+11.0 ± 0.2
CS + dp10 1:0.4	6471 ± 545	0.630	+1.7 ± 0.1
CS + dp10 1:1	2710 ± 1224	0.897	-14.6 ± 0.2
CS + dp10 1:1.8	337.6 ± 3.5	0.369	-21.6 ± 0.3
CS + dp10 1:3.6	6584 ± 2282	0.675	+0.5 ± 0.1
Starch + dp10 1:0.4	150.0 ± 1.4	0.077	-32.2 ± 1.7
Starch + dp10 1:3.6	128.9 ± 0.7	0.097	-34.7 ± 2.2
Starch + dp22 1:3.6	127.7 ± 0.4	0.106	-36.4 ± 2.4

Additionally, the approach of using smart excipients was followed by testing G-Blocks (guluronic acid oligomers, dp10 and dp22) for building the microparticle matrix. This material was evaluated for mucosal delivery of NPs and it could be shown that applying the G-Blocks together with NPs improved particle mobility in mucus due to a reduced mucus barrier function.[57, 45] The idea of additionally selecting G-Blocks as part of the microparticle preparation was that this could potentially improve bronchiolar uptake of particles that impact in the upper lung, where mucus is present as a non-cellular barrier. CS NPs showed signs of aggregating upon G-Block addition, with large particles between a few hundred nanometers up to the μm range being formed. From the ζ-potential values, which are often around 0±10 mV, it can be concluded that (partial) charge neutralization let to aggregation of the particles. An interaction between the positively charged surface of CS NPs and the negatively charged G-Blocks acids can be assumed. In contrast, starch NPs with added G-Blocks showed particles around or smaller than 150 nm with a PdI below 0.1 and a ζ-potential around -35 mV. Here, the NP suspension was not negatively influenced by aggregation, probably due to the fact, that both starch NPs and G-Blocks acids were negatively charged. Nevertheless, there was an influence of G-Blocks, as can be seen by the increase in ζ-potential magnitude from approximately -25 to -35 mV, indicating that G-Blocks might have been associated with the particle surface. As a conclusion, non-charged excipients for spray drying were favored, as they did not influence physicochemical properties of NPs.

A first result regarding powder properties after spray drying was powder flow ability, which differed for the various formulations. Although manni samples were more difficult to collect from the collecting electrode of the spray dryer, the powder flow appeared to be more regular compared to lact or treha samples – in these cases material was easy to remove from the electrode, however particles showed signs of aggregation during the collection process. Here, adhesion interaction between the particles was more pronounced than for manni samples. This is in accordance with literature data, in which manni has been reported to show good powder flowability.[56]

Release of Nanoparticles from Microparticles

The successful release of NPs from the microparticle matrix was one of the main requirements for the formulation. *In vivo,* this is an important point to be addressed, so it was the first parameter to be explored. The uptake of particles into cells is amongst other factors size dependent. For example, Desai et *al.* have shown that the uptake of NPs into Caco-2 cells is significantly greater compared to their microparticle counterparts.[41, 57] In general, it known that NPs in a size range between 100 - 200 nm are taken up by cells *via* endocytosis. Thus, NPs released from the microparticle matrix should have a size around or below 200 nm, and a narrow size distribution.

Figure 1: Dissolution behavior of microparticles, and comparison of physicochemical properties of NPs before spray drying and after being released from the microparticles. (A)

CS NPs spray dried with different amounts of excipient. (B) Starch NPs spray dried with different amounts of excipient.

In a proof of concept study, approximately 1 mg each of the microparticle formulations was dissolved in 1 mL aqueous solution and vortexed for 10 s (to speed up the dissolution process). Released NPs were measured for their size and size distribution. Results for different formulations can be found in Figure 1, where CS NP formulations are shown in and starch NP formulations are shown in (B). It could be seen that blank NPs, spray dried without excipient, were not able to be redispersed. This was the case for CS NPs, which showed aggregates in the µm size range and a PdI close to 1. Compared to that, starch NPs showed an improved behavior, nevertheless, the size distribution was not satisfactory. During the drying process, the gel-like NPs probably came into contact with each other, forming larger particles.
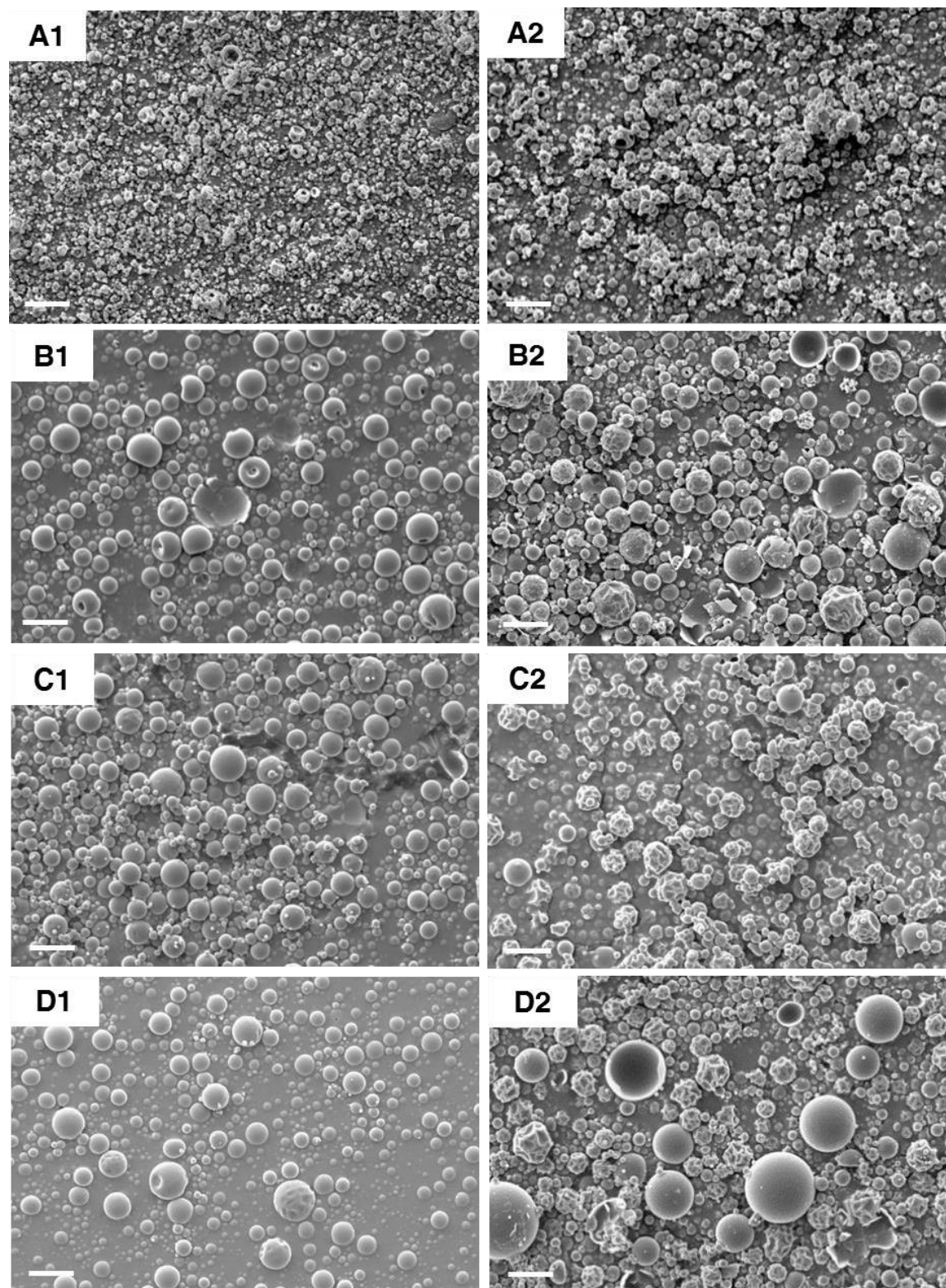
Adding different excipients in a mass ratio 1:5 (NP: excipient) could not improve the redispersion behavior of both NP types. However, a mass ratio of 1:20 led to a good redispersion of NPs with physicochemical properties being similar to the NP suspension before spray drying. The excipient served as drying protectant, probably due to steric hindrance, so that the NPs were not able to merge into larger particles. One exception is manni, which could still not improve the dissolution behavior of CS NPs in a mass ratio of 1:20. Loaded starch NPs with 150 µL IgG1 solution (5 mg/mL) also showed a good redispersion when spray dried with treha in a mass ratio NP: excipient of 1:20. The size of these loaded NPs after redispersion was 243.0 ± 9.2 nm with a PdI of 0.2.

As a result, a mass ratio of 1:20 NP: excipient was chosen for further experiments. The material of choice was determined to be manni or treha, showing good protection of the NP suspension during spray drying.

Morphology

The morphology of all spray dried samples was examined using SEM. Representative images of spray dried NPs without excipient and with excipient in a mass ratio of 1:20 (NP: excipient) are shown in Figure 1.2. It could be seen that both types of NPs, when spray dried without excipient, were very small and had an undefined shape. In contrast, NPs spray dried with excipient were larger and of defined shape. Depending on the kind of NP, the morphology differed: microparticles prepared from CS NPs spray dried with different excipients had a spherical and smooth surface, whereas starch NPs spray dried with excipient additionally had wrinkled shapes.
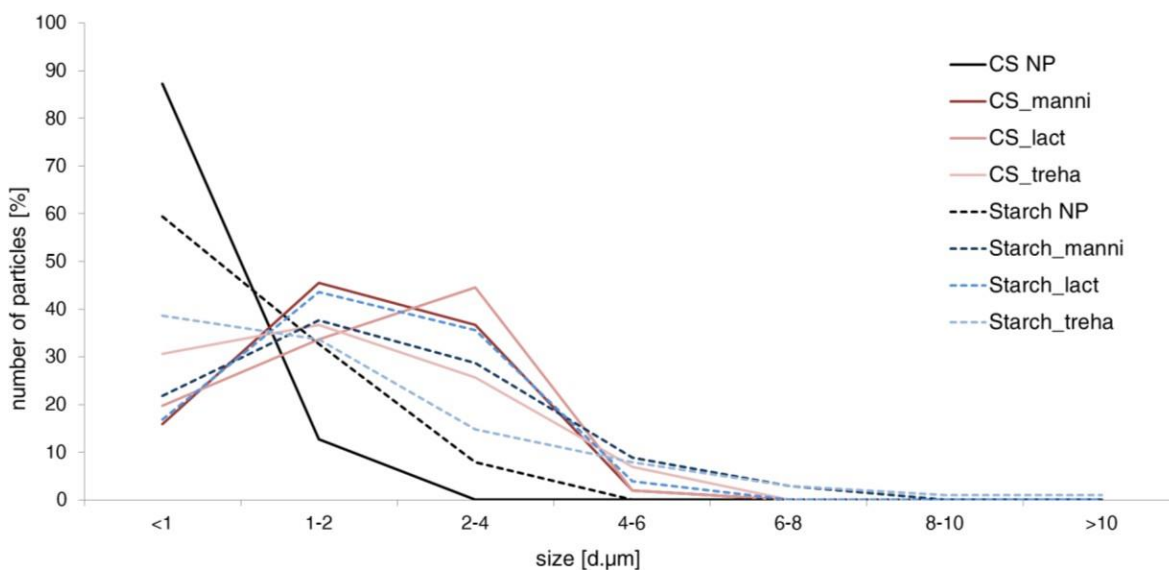
Figure 2: SEM images of spray dried NPs without (A) or with 1:20 excipient: manni (B) lact (C) treha (D); column on the left: CS NPs (1); column on the right: starch NPs (2); scale bar: 1 μm.

Iskandar et al. have shown that morphology of spray dried particles depends on parameters such as droplet size of the material to be spray dried, viscosity of the droplet, size of the sol in the droplet,

drying temperature, gas flow rate and addition of surfactant. From a theoretical perspective they concluded that the structural stability of the droplet and the hydrodynamic effects during the drying process might play important roles in controlling the morphology of the resulting particles.188 As spray drying parameters, such as droplet size (determined by the spray cap), gas flow rate and drying temperature was kept constant, the differences in morphology are likely chiefly influenced by formulation parameters in this case.

Spray drying of blank NPs led to a collapse of the droplet during the drying process, resulting in particles of undefined shape. Adding an excipient, however, increased the mass fraction in the droplet, stabilizing the droplet due to its internal stiffness, meaning that prepared particles showed a more defined shape and were almost spherical. A review from Vehring presented a classification based on dimensionless numbers (*e.g.* Peclet number) that can be used to estimate how excipient properties in combination with process parameters influence the morphology of engineered particles.[59] The differences in shape of microparticles have to do with the NP type, as process parameters and excipients were kept constant. It could be assumed that starch NPs have a different Peclet number compared to CS NPs, resulting in a different diffusion behavior in the droplet, leading to a different particle shape.
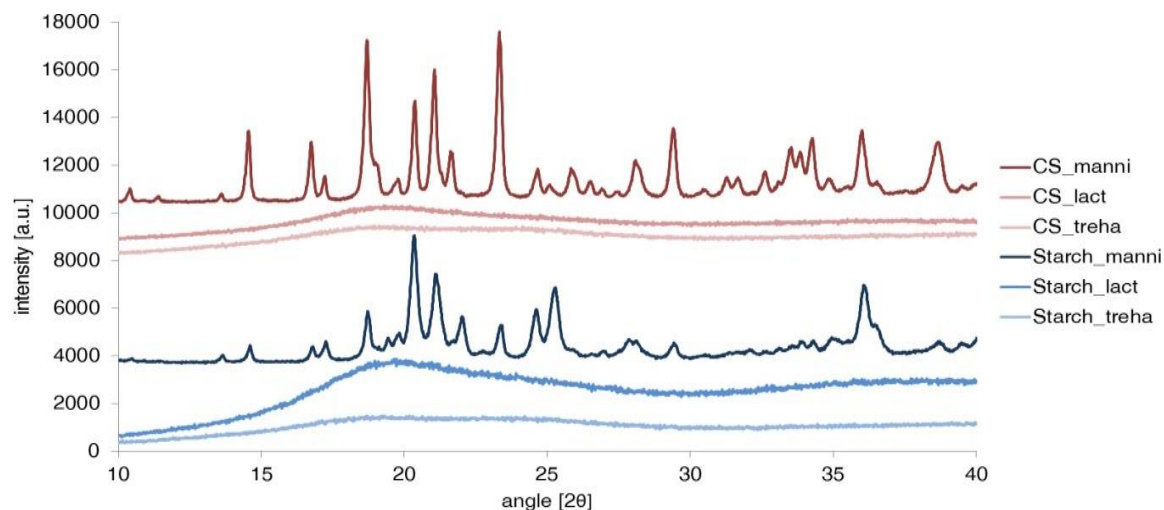
Particle Size and Particle Size Distribution

Figure 3: Particle size distribution of optimized microparticles spray dried with various excipients, compared to NPs, spray dried without excipient.
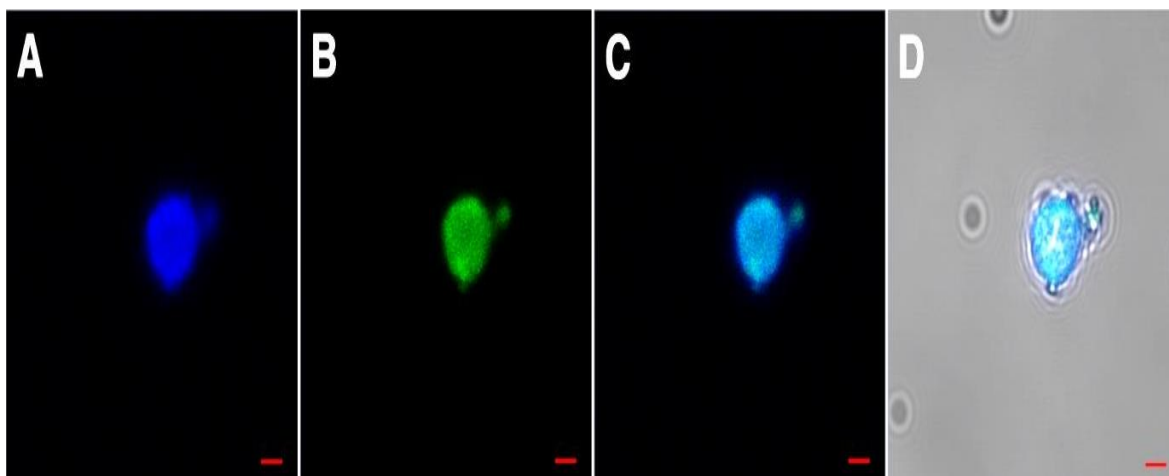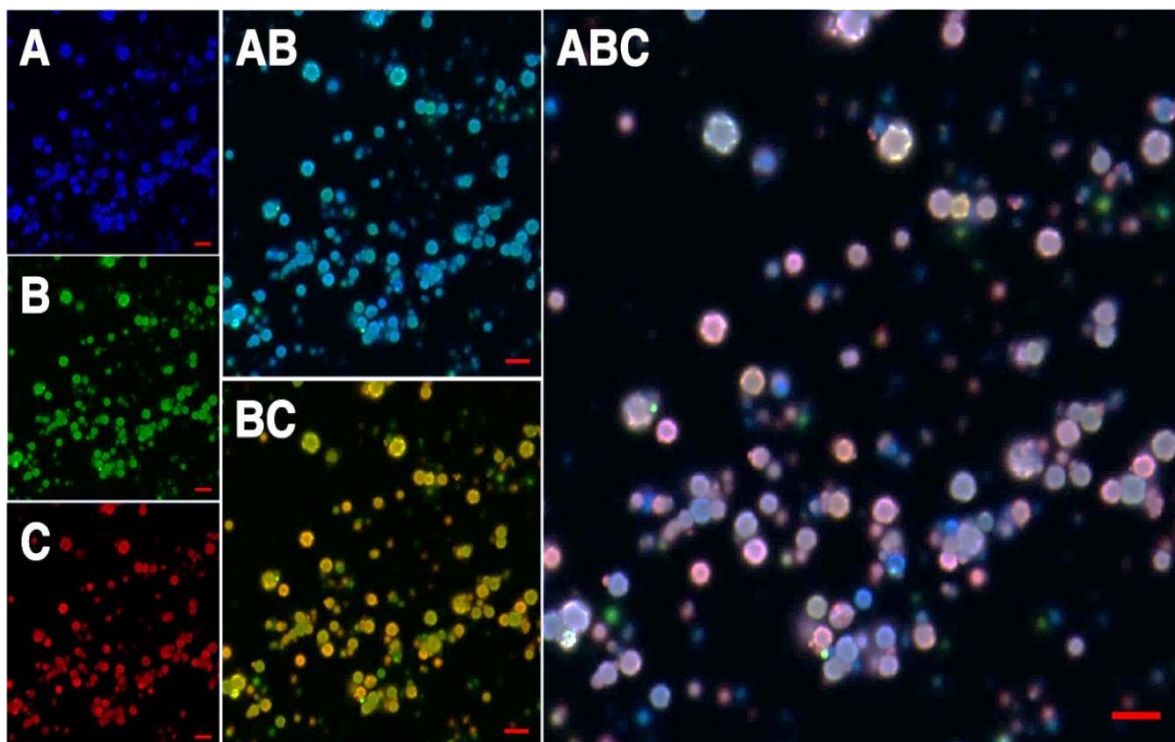
Powder Crystallinity

Figure 5: XRPD diffractograms of microparticles

LOCALIZATION OF NANOPARTICLES IN MICROPARTICLES

Figure 6: Confocal images of labeled starch NPs (green), co-spray dried with treha (mass ratio 1:20) and DAPI (blue). (A) DAPI, representing the microparticle matrix, (B) Bodipy (green label), representing the NPs; (C) fluorescence overlay; (D) additional overlay with light microscopic image; scale bar: 2 μm.

Figure 7: Fluorescence images of labeled starch NPs, loaded with labeled IgG1 and co- spray dried with treha (mass ratio 1:20) and DAPI.

(A) DAPI, representing the microparticle;

(B)Bodipy, representing the nanoparticles; (C) Alexa Fluor 647, representing IgG1; (AB) overlay of (A) and (B); (BC) overlay of (B) and (C); (ABC) overlay of (A), (B) and (C); scale bar: 10 μm.

CONCLUSION

Spray drying the NP suspension without excipient resulted in particles with an indistinct shape. Adding an excipient led to particles distinctly spherical in shape, with specific morphology depending mostly on the NP composition - spray dried CS samples with different excipients showed rather smooth and round surfaces, while spray dried starch samples with different excipients showed rather wrinkled shapes. NPs spray dried without excipient were not able to be redispersed. Depending on the amount of excipient, NPs were able to be redispersed in aqueous solution (mass ratio 1:20, NP: excipient).

The particle size distribution clearly depended on the specific excipient employed. Samples spray dried with manni showed the narrowest particle size distribution, whereas samples spray dried with lact or treha showed a broad size distribution.

Also crystallinity of the samples depended on the kind of excipient used. Manni samples showed a crystalline appearance after spray drying, whereas lact and treha samples were completely amorphous.

The internal structure of the microparticles was evaluated by confocal fluorescence microscopy, using the formulation of Starch_treha (loaded with IgG1) as model formulation to get an idea of whether the NPs are located at the surface, or rather spread throughout the excipient matrix. It was seen that the latter phenomenon occurred with starch NPs being present throughout the entire microparticle and not only at the surface. The same was true for the formulation loaded with IgG1. In summary, taking into consideration all tested excipients, there is no clear advantage of one special excipient. Lact and treha showed a good redispersion behavior of NPs, however their amorphous and highly cohesive character was detrimental for their delivery to the deep lung. Manni showed a high degree of deposition and good redispersion in the case of starch NPs, however, its influence on protein stability has to be further evaluated. A mixture of treha and manni as matrix builder for the microparticle preparation could be proposed. Assessing the NP type, starch NPs clearly show an advantage for both important parameters - redispersion of the NPs after microparticle dissolution and high deposition in the deep lung - compared to CS NPs.

REFERENCES

1. Patton, J. S., and Byron, P. R. (2007), Inhaling medicines: delivering drugs to the body through the lungs. *Nature reviews. Drug discovery 6,* 67-74.

2. Geiser, M., Rothen-Rutishauser, B*., et al.* (2005), Ultrafine particles cross cellular membranes by nonphagocytic mechanisms in lungs and in cultured cells. *Environmental health perspectives 113*, 1555-1560.

3. Herd, H., Daum, N*., et al.* (2013), Nanoparticle geometry and surface orientation influence mode of cellular uptake. *ACS nano 7,* 1961-1973.

4. Ruge, C. A., Kirch, J*., et al.* (2011), Uptake of nanoparticles by alveolar macrophages is triggered by surfactant protein A. Nanomedicine : nanotechnology, biology, and medicine 7, 690-693.

5. Ruge, C. A., Schaefer, U. F., et al. (2012), The interplay of lung surfactant proteins and lipids assimilates the macrophage clearance of nanoparticles. PloS one 7, e40775.

6. Patton, J. S., Brain, J. D., et al. (2010), The particle has landed--characterizing the fate of inhaled pharmaceuticals. Journal of aerosol medicine and pulmonary drug delivery 23 Suppl 2, S71-87.

7. Lai, S. K., O'Hanlon, D. E*., et al.* (2007), Rapid transport of large polymeric nanoparticles in

fresh undiluted human mucus. Proceedings of the National Academy of Sciences of the United States of America 104, 1482-1487.

8. Mura, S., Hillaireau, H., et al. (2011), Biodegradable Nanoparticles Meet the Bronchial Airway Barrier: How Surface Properties Affect Their Interaction with Mucus and Epithelial Cells. Biomacromolecules 12, 4136-4143.

9. Nordgård, C. T., Nonstad, U., et al. (2014), Alterations in Mucus Barrier Function and Matrix Structure Induced by Guluronate Oligomers. Biomacromolecules 15, 2294-2300.

10. Hasenberg, M., Stegemann-Koniszewski, S., et al. (2013), Cellular immune reactions in the lung. Immunol Rev 251, 189-214.

11. Todoroff, J., and Vanbever, R. (2011), Fate of nanomedicines in the lungs. Current Opinion in Colloid & Interface Science 16, 246-254.

12. Brand, P., Schulte, M., et al. (2009), Lung deposition of inhaled alpha1-proteinase inhibitor in cystic fibrosis and alpha1-antitrypsin deficiency. The European respiratory journal 34, 354-360.

13. Heyder, J. (2004), Deposition of inhaled particles in the human respiratory tract and consequences for regional targeting in respiratory drug delivery. Am Thorac Soc 1, 315-320.

14. Ely, L., Roa, W., et al. (2007), Effervescent dry powder for respiratory drug delivery.

15. European Journal of Pharmaceutics and Biopharmaceutics 65, 346-353.

16. Tsapis, N., Bennett, D., et al. (2002), Trojan particles: large porous carriers of nanoparticles for drug delivery. Proceedings of the National Academy of Sciences of the United States of America 99, 12001-5.

17. Pillai, O., and Panchagnula, R. (2001), Polymers in drug delivery. Current Opinion in Chemical Biology 5, 447-451.

18. Kumari, A., Yadav, S. K., et al. (2010), Biodegradable polymeric nanoparticles based drug delivery systems. Colloids and Surfaces B: Biointerfaces 75, 1-18.

19. Houchin, M. L., and Topp, E. M. (2008), Chemical degradation of peptides and proteins in PLGA: A review of reactions and mechanisms. Journal of Pharmaceutical Sciences 97, 2395-2404.

20. Germershaus, O., Lühmann, T., et al. (2015), Application of natural and semi-synthetic polymers for the delivery of sensitive drugs. International Materials Reviews 60, 101-131.

21. Dang, J., and Leong, K. (2006), Natural polymers for gene delivery and tissue engineering.

22. Advanced Drug Delivery Reviews 58, 487-499.

23.   Pereswtoff-Morath, L., and Edman, P. (1995), Dextran microspheres as a potential nasal drug delivery system for Paclitaxel - in vitro and in vivo properties. International Journal of Pharmaceutics 124, 37-44.

24.   Chiu, H.-C., Hsiue, G.-H., et al. (1999), Synthesis and characterization of pH-sensitive dextran hydrogels as a potential colon-specific drug delivery system. Journal of Biomaterials Science, Polymer Edition 10, 591-608.

25.   Hovgaard, L., and Bronsted, H. (1995), Dextran hydrogels for colon-specific drug delivery.

26. Journal of Controlled Release 36, 159-166.

27.   Rajaonarivony M., Vauthier C., et al. (1993), Development of a new drug carrier made from alginate. Journal of Pharmaceutical Sciences 82, 912-917.

28.   Calvo, P., Remunan-Lopez, C., et al. (1997), Novel hydrophilic chitosan-polyethylene oxide nanoparticles as protein carriers. Journal of Applied Polymer Science 63, 125-132.

29.   Grenha, A., Grainger, C. I., et al. (2007), Chitosan nanoparticles are compatible with respiratory epithelial cells in vitro. European Journal of Pharmaceutical Sciences 31, 73-84.

30.   Coppi, G., Iannuccelli, V., et al. (2001), Chitosan-alginate microparticles as a protein carrier. Drug Development and Industrial Pharmacy 27, 393-400.

31.   James, K. A., Fresneau, M. P., et al. (2001), Chitosan nanoparticles as delivery systems for doxorubicin. Journal of Controlled Release 73, 255-267.

32.   Günbeyaz, M., Faraji, A., et al. (2010), Chitosan based delivery systems for mucosal immunization against bovine herpesvirus 1 (BHV-1). European Journal of Pharmaceutical Sciences 41, 531-545.

33.   Ingram, J. T., and Lowenthal, W. (1966), Mechanism of Action of Starch as a Tablet Disintegrant I - Factors that Affect the Swelling of Starch Grains at 37°. Journal of Pharmaceutical Sciences 55, 614-617.

34.   Patel, N. R., and Hopponen, R. E. (1966), Mechanism of Action of Starch as a Disintegrating Agent in Aspirin Tablets. Journal of Pharmaceutical Sciences 55, 1065-1068.

35.   Kitamori, N., and Makino, T. (1982), Improvement in Pressure-Dependent Dissolution of Trepibutone Tablets by Using Intragranular Disintegrants. Drug Development and Industrial Pharmacy 8, 125-139.

36.   Kottke, M. K., Chueh, H. R., et al. (1992), Comparison of Disintegrant and Binder Activity of Three Corn Starch Products. Drug Development and Industrial Pharmacy 18, 2207-2223.

37.   Callens, C., Ceulemans, J., et al. (2003), Rheological study on mucoadhesivity of some nasal

powder formulations. European Journal of Pharmaceutics and Biopharmaceutics 55, 323-328.

38. Clausen, A. E., and Bernkop-Schnürch, A. (2001), Direct compressible polymethacrylic acid-starch compositions for site-specific drug delivery. Journal of Controlled Release 75, 93-102.

AJPTR is

- **Peer-reviewed**
- **bimonthly**
- **Rapid publication**

Submit your manuscript at: editor@ajptr.com